Ultraflat broadband supercontinuum in highly nonlinear $Ge_{11.5}As_{24}Se_{64.5}$ photonic crystal fibres

[1]Sandeep Vyas, [2]Takasumi Tanabe, [3]Manish Tiwari and [4]Ghanshyam Singh

[1] Dept. of ECE, Vivekananda Institute of Technology, Jaipur, India, vyas.sandeep@vitej.ac.in

[2] Dept. of EEE, Keio University, Kanagawa, Japan, takasumi@elec.keio.ac.jp

[3] Dept. of ECE, Manipal University, Jaipur, India, manishtiwari@ieee.org

[4] Dept. of ECE, Malaviya National Institute of Technology, Jaipur, India, gsingh.ece@mnit.ac.in

Abstract: We demonstrate numerically a possible generation of a mid-infrared (1–10 μm) supercontinuum, using highly nonlinear $Ge_{11.5}As_{24}Se_{64.5}$-based photonic crystal fibres. This ultra-broadband supercontinuum is achieved with a 100 mm long photonic crystal fibre pumped using 85 fs laser pulses at 3.1 μm with the peak power 3 kW. A broad and flat dispersion profile of the $Ge_{11.5}As_{24}Se_{64.5}$-based photonic crystal fibre combined with a high nonlinearity result in the hyper-broadband supercontinuum.

1. Introduction

Nowadays photonic crystal fibres (PCFs) have proven their importance in the fields of communications, biomedical applications and sensor technologies. PCFs have a microscopic array of air holes around the core that runs along the entire fibre length, thus offering design flexibility in tailoring dispersion slope and nonlinearity [1]. One of their recent applications is super-continuum generation (SCG). This is a phenomenon in which an ultrashort laser pulse undergoes extreme nonlinear spectral broadening to produce a broadband, spectrally continuous output as a result of interplay between higher-order dispersion and various nonlinear processes. Many applications such as optical coherence tomography, spectroscopy, frequency metrology and wavelength conversion can be achieved with the SCG. Wavelength-division multiplexing is still another useful application of the phenomenon [3]. The PCFs play an important role in implementing the SCG because of reduced input power requirements. This can be achieved by reducing the effective area and enhancing the nonlinear properties of the PCFs [2].

Besides of silica, non-silica materials can also be used as a background material for the PCFs. This often results in interesting optical properties of the PCFs due to unique properties of the underlying materials. An important property is nonlinearity, which governs the spectral broadening of optical pulses and can be maximized by tailoring the effective area and/or by selecting materials with higher nonlinear Kerr coefficients [4]. In particular, chalcogenide glasses have a number of incomparable properties that make them desirable for fabricating planar optical waveguides and for implementing SCG in the mid-infrared range [5]. These glasses are optically transparent in the

mid-infrared, with the transparency region reaching beyond 8.5 μm for sulphides, 14 μm for selenides and around 20 μm for tellurites [6]. Some of the chalcogenide materials like As_2S_3, As_2Se_3, $Ge_{11.5}As_{24}S_{64.5}$ and $Ge_{11.5}As_{24}Se_{64.5}$ are tremendously suitable for making both active and passive optoelectronic devices for the mid-infrared. Amomg different chalcogenides, $Ge_{11.5}As_{24}Se_{64.5}$ has drawn much attention of researchers owing to its high thermal and optical stability and excellent film-forming properties under intense illumination [7].

As long ago as in 2010 Xin Gai et al. [8] have fabricated 600×500 nm^2 nanowires from $Ge_{11.5}As_{24}Se_{64.5}$ for utilizing in the SCG in the light wavelength region from 1000 to 2200 nm. With a 18 mm long nanowire they have obtained a sufficiently high nonlinear coefficient, $\gamma \approx 136 \pm 7$ W^{-1}m^{-1} at 1550 nm. M. Spurny et al. [9] have demonstrated a number of techniques for fabricating PCFs based on the $Ge_{11.5}As_{24}Se_{64.5}$ chalcogenide glass. M. R. Karim et al. [10] have simulated numerically the relevant results obtained with five different nanowire structures, of which widths range from 700 to 800 nm. The supercontinuum spanning up to 4600 nm has been achieved. Very recently, Panarit Sakunasinha et al. [11] have reported the results of simulations for $Ge_{11.5}As_{24}Se_{64.5}$ combined with MgF_2 as a lower cladding and achieved the SCG from 1300 to 3300 nm with 1 cm long fibres. Finally, M. R. Karim et al. [12] have reported some results with microstructured fibres and achieved the spectrum extending from 1.3 μm to beyond 11 μm.

The present work is organized as follows. Section 2 analyzes concisely the modal properties of $Ge_{11.5}As_{24}Se_{64.5}$-based chalcogenide PCFs. In particular, we calculate the second-order Sellmeier formula for this material, while our more complete modal study of the optical parameters of the PCF involves the refractive index, the chromatic dispersion, the effective area and the nonlinear coefficient. In Section 3 we present the main results obtained for the SCG effect in a few-millimetre chalcogenide PCF based on $Ge_{11.5}As_{24}Se_{64.5}$. Finally, we use a generalized nonlinear Schrödinger equation to examine the SCG effect in a much detail.

2. Methods of analyses

We use a finite-difference time-domain method to analyze the optical properties of the PCFs. The total dispersion or the chromatic dispersion D_c can be calculated using the relationship

$$D_c(\lambda) = -\frac{\lambda}{c} \frac{d^2 n_{eff}}{d\lambda^2} , \qquad (1)$$

where λ is the operating wavelength, c the speed of light in vacuum, and n_{eff} the real part of the effective index ($n_{eff} = \lambda\beta/2\pi$, with β being the propagation constant) [2]. The wavelength-dependent refractive index of the $Ge_{11.5}As_{24}Se_{64.5}$ chalcogenide is given by the Sellimeier equation [13]:

$$n^2(\lambda) = 1 + \frac{5.78525\lambda^2}{\lambda^2 - 0.28795^2} + \frac{0.39705\lambda^2}{\lambda^2 - 30,39338^2} , \qquad (2)$$

where the wavelength λ is in the units of microns. The nonlinear coefficient γ is evaluated as [2]

$$\gamma = \frac{2\pi n_2}{\lambda A_{eff}} , \qquad (3)$$

where n_2 denotes the nonlinear refractive index of the material, λ the pump wavelength, and A_{eff} the effective area of the fundamental mode. Notice that the chalcogenide glass $Ge_{11.5}As_{24}Se_{64.5}$ is characterized by the index $n_2 = 4.3 \times 10^{-18}$ m^2/W at 3.1 μm [7]. The effective area A_{eff} of the propagating mode in the PCF is calculated using the formula [2]

$$A_{eff} = \frac{\left(\iint\limits_{-\infty}^{\infty} |E|^2 \, dxdy\right)^2}{\iint\limits_{-\infty}^{\infty} |E|^4 \, dxdy} \,,$$

(4)

where the function E describes the electric field distribution. Finally, the confinement loss CL is calculated using the relation $CL = 8.686 k_0 \mathrm{Im}(n_{eff})$ [2], where $\mathrm{Im}(n_{eff})$ implies the imaginary part of the effective refractive index and $k_0 = 2\pi/\lambda$ the free-space wave number [14].

The pulse propagation in the PCFs may be described numerically with a generalized nonlinear Schrödinger equation. Using a split-step Fourier method and denoting the output optical pulse envelop as $A(z, t)$, this equation may be rewritten as

$$\frac{\partial A}{\partial z} + \frac{\alpha}{2} A - \left(\sum_{n \geq 2} \beta_n \frac{t^{n+1}}{n!} \frac{\partial^n A}{\partial t^n}\right) = i\gamma \left(1 + \frac{i}{\omega_0} \frac{\partial}{\partial t}\right) \left[A(z,t) \int\limits_{-\infty}^{\infty} R(t') |A(z, t - t')|^2 \, dt'\right],$$

(5)

where α is the linear loss, t the time, t' the present time frame, z the distance, β_n the n-th derivative of the propagation constant β, R the nonlinear response function, and ω_0 the input pulse frequency (see Ref. [2]).

The Raman response function of the material that includes both instantaneous electronic and vibrational contributions is described as [2]

$$R(t) = (1 - f_r)\delta(t) + f_r h_R(t)`\,,$$

(6)

where f_r represents the fraction of $h_R(t)$ and $h_R(t)$ is the temporal Raman response. It depends upon the Raman gain spectrum that can be expressed as (see [15])

$$g_R(f) = \frac{2\omega_p}{c} n_2 f_r \mathrm{Im}\left[H_R(f)\right],$$

(7)

where ω_p denotes the pump frequency and $\mathrm{Im}[H_R(f)]$ the imaginary part of the Fourier transform of $h_R(t)$ [7]. The characteristics $h_R(t)$ is calculated as

$$h_R(t) = \frac{\tau_1^2 + \tau_2^2}{\tau_1 \tau_2^2} \exp\left(-\frac{t}{\tau_2}\right) \sin\left(\frac{t}{\tau_1}\right),$$

(8)

where we have $\tau_1 = 15.5$ fs and $\tau_2 = 230.5$ fs for the $Ge_{11.5}As_{24}Se_{64.5}$-based glass. One can find the fraction f_r using the Kramers–Kronig relation [14]

$$f_r = \frac{\lambda}{2\pi^2 n_2} \int\limits_0^{\infty} \frac{g_R(f)}{f} \, df \,.$$

(9)

It is equal to 0.031 [7].

Finally, we consider a hyperbolic secant pulse as an input. It may be expressed as

$$A(z = 0, t) = \sqrt{P_0} \, \mathrm{sec}\,h\left(\frac{t}{t_0}\right) \exp\left(-i\frac{C}{2}\frac{t^2}{t_0^2}\right),$$

(10)

where C is the chirp parameter, P_0 the peak power of the input pulse, $t_0 = t_{\mathrm{FWHM}}/1.7627$, and t_{FWHM} implies the full width of the pulse at its half-maximum.

3. PCF design and analysis

As already mentioned above, the $Ge_{11.5}As_{24}Se_{64.5}$-based chalcogenide PCFs are the best choice for implementing SCG because of very high nonlinearity coefficient γ. We have designed a

134

Ukr. J. Phys. Opt. 2016, Volume 17, Issue 3

$Ge_{11.5}As_{24}Se_{64.5}$-based PCFs, which are suitable for the SCG with 3.1 μm pumping. The dispersion has been tailored very carefully to achieve the desirable dispersion characteristics. The cross sections of our PCFs are displayed in Fig. 1. Here analyze five-ring hexagonal PCF structures. The parameters of the three PCFs designed in the present work, which are denoted as PCF-1, PCF-2, PCF-3, are shown in Table 1.
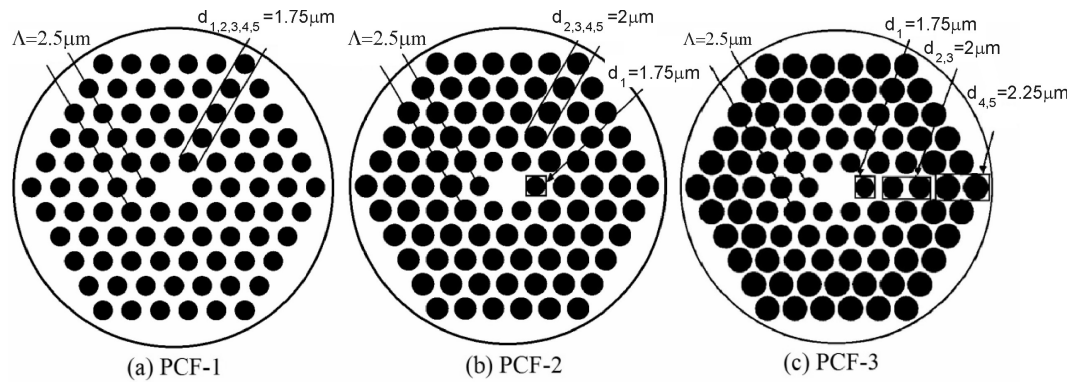

Fig. 1. Structure of our PCFs with hexagonal cladding of air holes.

Table 1. Design parameters of our PCFs (see the text).

Fibre	Number of rings	Pitch Λ, μm	d_1/Λ	d_2/Λ	d_3/Λ	d_4/Λ	d_5/Λ
PCF-1			0.7				
PCF-2	5	2.5	0.7	0.8			
PCF-3			0.7	0.8		0.9	

To study the dispersion in a more detail, we have calculated dependences of the effective refractive index n_{eff} of the fundamental mode on the operating wavelength λ (see Fig. 2). The data displayed in Fig. 2 demonstrate the effect of variations in the pitch and the air hole size on the effective refractive index. Notice that all of our PCFs are based on the five-ring structure with the constant pitch ($\Lambda = 2.5$ μm). The sizes of the first-ring air holes are denoted as d_1 and so on, so that the size d_5 corresponds to the last-ring air holes. We have $d/\Lambda = 0.7$ for PCF-1, $d_1/\Lambda = 0.7$ and $d_{2,3,4,5}/\Lambda = 0.8$ for PCF-2, and $d_1/\Lambda = 0.7$, $d_{2,3}/\Lambda = 0.8$ and $d_{4,5}/\Lambda = 0.9$ for PCF-3. As seen from Fig. 2, the effective refractive index decreases with increasing diameter of the air holes. In other words, the increase in the air hole diameter reduces the index contrast between the core and the cladding and, therefore, the effective refractive index value becomes smaller [16].

The spectral dependences of the chromatic dispersion for our fibres are shown in Fig. 3. By carefully choosing the pitch Λ and the air-hole diameter d, one finds a flat dispersion profile from about 2.7 to 10 μm, with two zero-dispersion wavelength points. The SCG can be maximized by achieving a low flat dispersion profile. This reduces temporal walk-off effect during spectral boarding process [17]. It is worthwhile that the pumping wavelength (3.1 μm) is located in the region of anomalous dispersion for the all PCFs. The solid line in Fig. 3 shows the material dispersion for the $Ge_{11.5}As_{24}Se_{64.5}$ glass. Note that the n_{eff} value decreases monotonically when one passes from PCF-3 to PCF-1 (see Fig. 2). Moreover, as seen from Fig. 3, the chromatic dispersion curve becomes less flatter under the same conditions. In other terms, a decrease in the n_{eff} value is accompanied by flattening of the dispersion curve. The zero-dispersion wavelengths of our PCFs are summarized in Table 2, along with the corresponding parameter of the material dispersion.
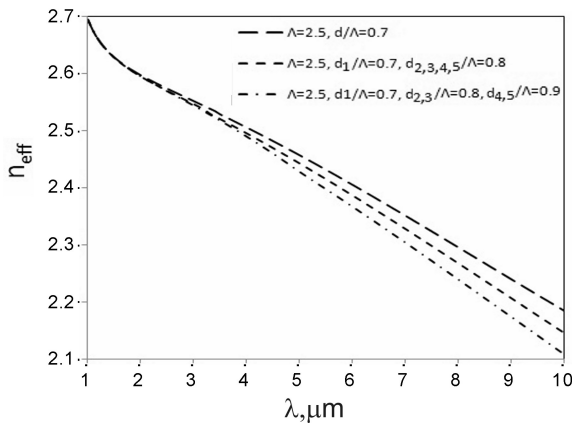
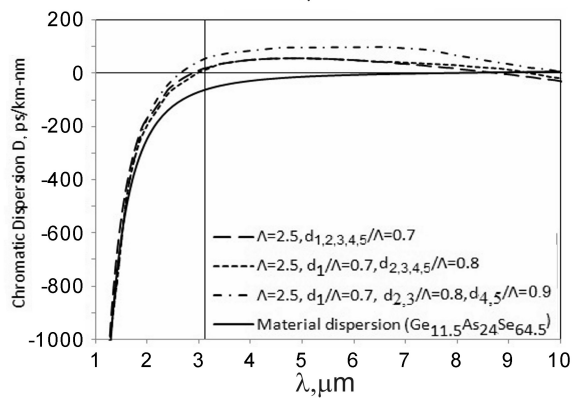**Fig. 2.** Effective refractive indices of our PCFs.


Fig. 3. Chromatic dispersion for our PCFs.

Table 2. Dispersion parameters of our PCFs: ZDW-1 and ZDW-1 abbreviate the two zero-dispersion wavelengths available for the PCFs.

| Fibre or material	ZDW-1, μm	ZDW-2, μm
PCF-1	2.85	8.90
PCF-2	2.87	9.50
PCF-3	2.70	10.0
Material	7.10	–

4. SCG effect in our PCFs

As mentioned above, we have simulated the SCG phenomenon in our PCFs via solving the generalized nonlinear Schrödinger equation with the split-step Fourier method [18]. The PCF length has been fixed at 100 mm. We have chosen the fibre PCF-3 for the SCG simulations since it provides the maximum flatness of the dispersion curve. The pumping optical pulses at 3.1 μm are assumed to have a hyperbolic secant shape. The calculations have yielded the following parameters: $A_{eff} = 3.7634 \ \mu m^2$, $\gamma = 2317 \ W^{-1}km^{-1}$ and $CL = -1.5209 \times 10^{-7} \ dB/km$ (at the pump wavelength of 3.1 μm). This wavelength is located in the region of anomalous dispersion, with the 'flat region' ranging from 2.7 to 10 μm. In the anomalous regime, the primary broadening originates from four-wave mixing. Further propagation increases the spectral broadening in the long-wavelength region. This is mainly caused by Raman soliton self-frequency shift and soliton fission, as well as by generation of dispersive waves on the short-wavelength side of the zero-dispersion wavelength points, which eventually merge to a broad supercontinuum spectrum [17]. The pulse duration defined as FWHM is equal to 85 fs and the peak power to 3 kW. The spectral

spans of the SCG found for the case of PCF-3 are shown in Fig. 4. Finally, the spectral escalation of supercontinuum obtained for different fibre lengths is displayed in Fig. 5.
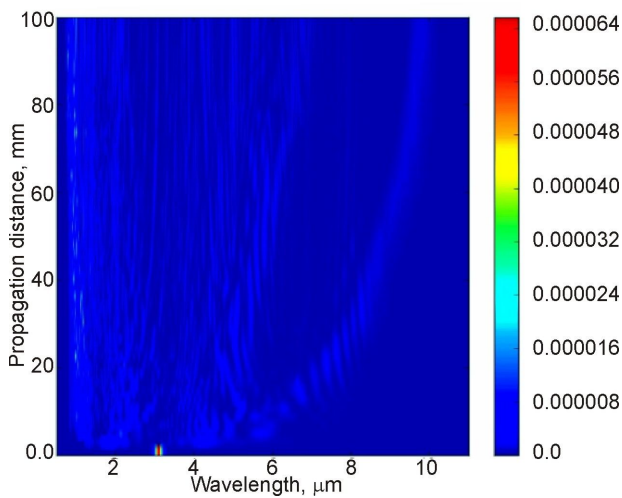
Fig. 4. Spectral escalation of supercontinuum in PCF-3
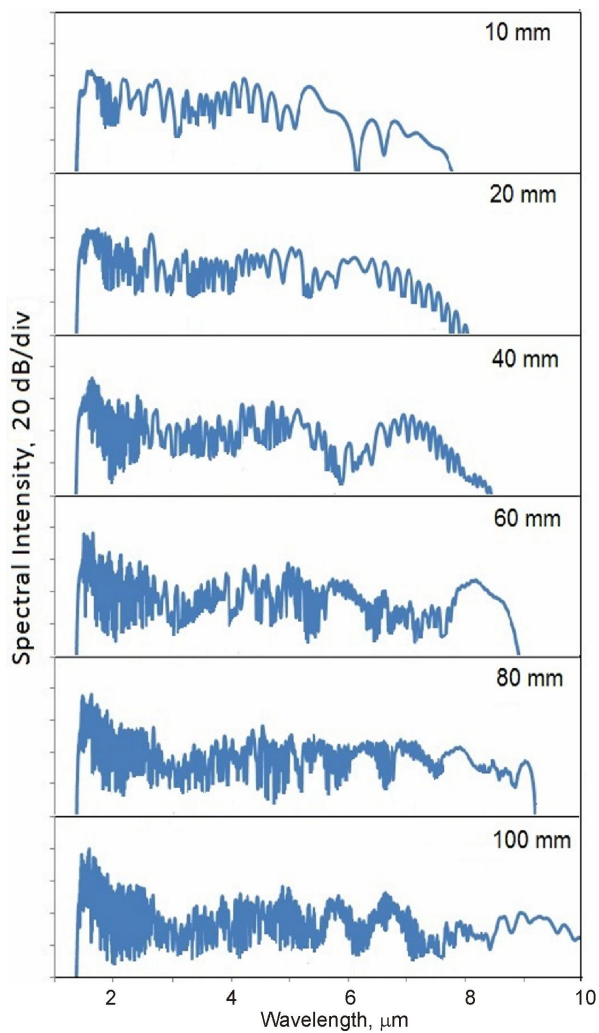
Fig. 5. Spectra of supercontinuum for the PCFs of different lengths

5. Conclusion

Using the techniques of numerical modelling, we have demonstrated a possibility for the SCG effect in the 100 mm long solid-core PCF based on the $Ge_{11.5}As_{24}Se_{64.5}$ glass. Our PCF has a hexagonal cladding of the air holes. We have designed three different PCFs and achieved a flat-dispersion region as wide as 2–10 μm. For the case of fibre denoted as PCF-3, the nonlinear coefficient γ, the effective area A_{eff} and the dispersion at 3.1 μm have been calculated. They are equal to 2317 $W^{-1}km^{-1}$, 3.7634 $μm^2$ and 52 ps/km/nm, respectively. Our PCFs have been numerically simulated for the purpose of SCG, using 85 fs pumping pulses with the peak power 3 kW and the wavelength 3.1 μm. The supercontinuum so generated ranges from 1 to 10 μm.

Acknowledgment

References

1. Vyas S, Singh G, Tiwari M and Tanabe T, 2015. Chalcogenide ($LiGSe_2$, LiGISe, $LiGaS_2$): A perfect material to design highly nonlinear PCFs for supercontinuum generation. Proc. ICRCWIP 2015. Springer Publication (2015), p. 409.

2. Agarwal G P. Nonlinear fiber optics, 4th ed. Rochester, NY: Academic Press, 2007.

3. Dudley J M, Genty G and Coen S, 2006. Supercontinuum generation in photonic crystal fibers. Rev. Mod. Phys. **78**: 1135–1184.

4. Tiwari M and Janyani V, 2011. Two-octave spanning supercontinuum in a soft glass photonic crystal fiber suitable for 1.55 μm pumping. J. Lighwave Technol. **29**: 3560–3565.

5. Gai X, Han T, Prasad A, Madden S, Choi DY, Wang R, Bulla D and Luther-Davies B, 2010. Progress in optical waveguides fabricated from chalcogenide glasses. Opt. Express. **18**: 26635–26646.

6. Eggleton B J, Luther-Davies B and Richardson K, 2011. Chalcogenide photonics. Nature Photon. **5**: 141–148.

7. Karim M R, Rahman B M A and Agrawal G P, 2015. Mid-infrared supercontinuum generation using dispersion-engineered $Ge_{11.5}As_{24}Se_{64.5}$ chalcogenide channel waveguide. Opt. Express. **23**: 6903–6914.

8. Gai X, Madden S, Choi D Y, Bulla D and Luther-Davies B, 2010. Dispersion engineered $Ge_{11.5}As_{24}Se_{64.5}$ nanowires with a nonlinear parameter of 136 $W^{-1}m^{-1}$ at 1550 nm. Opt. Express. **18**: 18866–18874.

9. https://research-repository.st-ndrews.ac.uk/bitstream/10023/2111/6/MarcelSpurnyPhDThesis.pdf.

10. Karim M R, Rahman B M A and Agrawal G P, 2014. Dispersion engineered $Ge_{11.5}As_{24}Se_{64.5}$ nanowire for supercontinuum generation: A parametric study. Opt. Express. **22**: 31029–31040.

11. Sakunasinha P, Suwanarat S and Chiangga S, 2015. Mid-infrared supercontinuum in a $Ge_{11.5}As_{24}Se_{64.5}$ chalcogenide waveguide. Proc. SPIE. **9659**: 96591J.

12. Karim M R, Rahman B M A, Azabi Y O, Agrawal A and Agrawal G P, 2015. Ultrabroadband mid-infrared supercontinuum generation through dispersion engineering of chalcogenide microstructured fibers. J. Opt. Soc. Amer. B. **32**: 2343–2351.

13. Vyas S, Tanabe T, Singh G, and Tiwari M. Broadband supercontinuum generation and Raman response in $Ge_{11.5}As_{24}Se_{64.5}$ based chalcogenide photonic crystal fiber. IEEE International Conference on Computational Techniques in Information and Communication Technologies. (2016), p. 607-611.

14. Poli F. Photonic crystal fibers. Properties and applications. Springer (2007).

15. Kartner F X, Dougherty D J, Haus H A and Ippen E P, 1994. Raman noise and soliton squeezing. J. Opt. Soc. Amer. B. **11**: 1267–1276.

16. Sharma M and Konar S, 2015. Three octave spanning supercontinuum by red-shifted dispersive wave in photonic crystal fibers. J. Mod. Opt. **63**: 501–510.

17. Yuan W, 2013. 2–10 μm mid-infrared supercontinuum generation in As_2Se_3 photonic crystal fiber. Laser Phys. Lett. **10**: 095107.

18. Mogilevtsev D, Birks T A and Russell P St J, 1999. Localized function method for modeling defect modes in 2-D photonic crystals. J. Lightwave Technol. **17**: 2078–2081.

Анотація. *У статті чисельно продемонстровано можливість генерації суперконтинууму в середньому інфрачервоному діапазоні 1–10 мкм із використанням фотонно-кристалічного оптичного волокна на основі високонелінійного $Ge_{11.5}As_{24}Se_{64.5}$. Цей ультра-широкосмуговий суперконтинуум досягається у фотонно-кристалічному волокні довжиною 100 мм при нагнітанні 85 фемтосекундними лазерними імпульсами з довжиною хвилі 3,1 мкм і піковою потужністю 3 кВт. Широкий і плоский профіль дисперсії фотонно-кристалічного волокна на основі $Ge_{11.5}As_{24}Se_{64.5}$ у поєднанні з його високою нелінійністю дає змогу генерувати гіперширокосмуговий суперконтинуум.*